

# Analytical Methods

Accepted Manuscript



This is an *Accepted Manuscript*, which has been through the Royal Society of Chemistry peer review process and has been accepted for publication.

*Accepted Manuscripts* are published online shortly after acceptance, before technical editing, formatting and proof reading. Using this free service, authors can make their results available to the community, in citable form, before we publish the edited article. We will replace this *Accepted Manuscript* with the edited and formatted *Advance Article* as soon as it is available.

You can find more information about *Accepted Manuscripts* in the [Information for Authors](#).

Please note that technical editing may introduce minor changes to the text and/or graphics, which may alter content. The journal's standard [Terms & Conditions](#) and the [Ethical guidelines](#) still apply. In no event shall the Royal Society of Chemistry be held responsible for any errors or omissions in this *Accepted Manuscript* or any consequences arising from the use of any information it contains.

1  
2  
3  
4  
5  
6  
7  
8  
9  
10  
11  
12  
13  
14  
15  
16  
17  
18  
19  
20  
21  
22  
23  
24  
25  
26  
27  
28  
29  
30  
31  
32  
33  
34  
35  
36  
37  
38  
39  
40  
41  
42  
43  
44  
45  
46  
47  
48  
49  
50  
51  
52  
53  
54  
55  
56  
57  
58  
59  
60

# The effect of acidity, hydrogen bond catalysis and auxiliary electrode reaction on the oxidation peak current for dopamine, uric acid and tryptophan

Yixuan Li, Jing Li, Enbo Shangguan\* and Quanmin Li\*

School of Chemistry and Chemical Engineering, Henan Normal University,  
Xinxiang, Henan, 453007, P.R. China

**Abstract:** A pre-anodized inlaying ultra-thin carbon paste electrode with 316L stainless steel as a matrix (316L-PAIUCPE) was prepared and employed for simultaneous determinations of dopamine (DA), uric acid (UA) and tryptophan (Trp). The influencing mechanism of acidity on the size of the oxidation peak currents ( $i_p$ ) for DA, UA and Trp were discussed from the aspects of the intensity of hydrogen bonding or electrostatic interactions between DA, UA, Trp and the negatively-charged functional groups at the surface of 316L-PAIUCPE, the degree of reduction reaction at the auxiliary electrode. Under the optimized experimental conditions, the oxidation peak currents increased linearly with the concentrations of DA, UA and Trp in the range of  $0.4\sim 200\ \mu\text{mol}\cdot\text{L}^{-1}$ ,  $0.5\sim 150\ \mu\text{mol}\cdot\text{L}^{-1}$  and  $0.1\sim 200\ \mu\text{mol}\cdot\text{L}^{-1}$ , respectively. The detection limits for DA, UA and Trp were found to be  $6.8\times 10^{-8}\ \text{mol}\cdot\text{L}^{-1}$ ,  $4.5\times 10^{-8}\ \text{mol}\cdot\text{L}^{-1}$  and  $5.3\times 10^{-8}\ \text{mol}\cdot\text{L}^{-1}$  in PBS buffer solution (pH=5.00), respectively. This method presented was successfully applied for determination of DA, UA, Trp in different samples.

**Keyword:** Hydrogen bond catalysis, Auxiliary electrode reaction, Dopamine, Uric acid, Tryptophan

---

\* Corresponding author. Tel.: +86 373 3326336; fax: +86 373 3326336.  
E-mail address: shangguanenbo@163.com (E. Shangguan); mercury6068@hotmail.com (Q. Li)

## Introduction

The different electrode materials will have a significant influence on the electrochemical behaviors of electroactive components.<sup>1</sup> Therefore, developing new electrode materials have attracted great interests in electroanalytical chemistry. For example, glassy carbon electrodes have attracted more and more attentions.<sup>2-4</sup> However, its preparation is complex and expensive. Similarly, carbon nanomaterials have also received great attention in recent years in different fields due to their enormous potential. Their remarkable electrical, chemical, mechanical and structural properties that make them a very attractive material for a wide range of applications. Their advantages such as good conductance, high surface area, favorable electronic properties and electrocatalytic effect make them adequate for the construction of electrochemical sensors and biosensors.<sup>5-11</sup> But their prices are expensive. The carbon paste electrode, due to the advantages such as its non-toxic, ease of modifying, rapid renewability and wide applicable potential range, has also been widely concerned by electroanalytical chemistry workers.<sup>12-13</sup> But it has a weakness: the analyte particles are easy to diffuse from the surface of the carbon paste electrode towards the inside, which will affect the reproducibility of determination.<sup>14</sup> In order to overcome this drawback, an inlaying ultra-thin (~ 100nm) carbon paste electrode (IUCPE) that adopts nichrome as a substrate is developed by Wang et al.,<sup>15</sup> which exhibits excellent performance, such as ease of making, low cost, high stability and good electrochemical response. 316L stainless steel is essentially a nickel-chromium-molybdenum alloy, which is used in shipbuilding industry<sup>16-17</sup> and also often used as femoral shaft.<sup>18</sup> In this work, a pre-anodized inlaying ultrathin carbon paste electrode (316L-PAIUCPE) is fabricated by using the industry leftover of 316L as substrate. Results show that neither 316L stainless steel nor nichrome can be used as the working electrode. However, after a ultra-thin carbon paste is inlaid at the surface of 316L stainless steel, a remarkable signal can be obtained for the redox of  $K_4[Fe(CN)_6]$ , and the dopamine (DA), uric acid (UA) and tryptophan (Trp) can be simultaneously determined. Compared with the literatures,<sup>19-23</sup> the electrode has its attractive advantages, such as ease of preparation, inexpensive and *so on*. Thus, it is easy to popularize in conventional laboratory and has a wide application prospect in the future.

1  
2  
3  
4  
5  
6  
7  
8  
9  
10  
11  
12  
13  
14  
15  
16  
17  
18  
19  
20  
21  
22  
23  
24  
25  
26  
27  
28  
29  
30  
31  
32  
33  
34  
35  
36  
37  
38  
39  
40  
41  
42  
43  
44  
45  
46  
47  
48  
49  
50  
51  
52  
53  
54  
55  
56  
57  
58  
59  
60

However, no matter what the working electrode is employed in the electroanalytical chemistry, the acidity of solution that has an important influence on the size of peak current and peak potential is always optimized as one of the preferential research conditions in general, especially, the electrode reaction that protons can be released in the process of electrode reaction. In fact, so far it had been not reported in detail to the mechanism for the effects of acidity on the size of peak current in the current literature. It is reported that the oxidation potentials of DA, UA and Trp always shift negatively with the pH increasing,<sup>24-27</sup> which means them to be more easily oxidized at the anode with the increase of pH, and then the oxidation current will be also enlarged. However, in fact, some of their oxidation peak currents always decrease with the pH rising, or increase at first and then decrease. It is simply reported to how the size of oxidation peak currents ( $i_{p,a}$ ) for DA, UA and Trp varies with pH value in literature<sup>28-31</sup>, the reasons that are related to the effect of pH on the size of peak current have not been theoretically explained in detail, therefore, it has an important significance to explore how the size of peak current is affected by the pH value.

In this paper, it is not only reported the method of simultaneous determination of DA, UA and Trp at 316L-PAIUCPE, but also discusses in detail the effect of pH on the size of  $i_{p,a}$  of DA, UA and Trp from the following aspects: 1) The degree of oxygen reduction reaction at the auxiliary electrode, 2) The oxidation peak potential and distribution coefficient of DA, UA and Trp, 3) The charge properties of electrode surface, 4) The formation and catalysis of hydrogen bond, 5) Their molecular configuration. It is shown that the losing electrons abilities for different acid-base species of DA, UA and Trp at electrode surface is one of the primary reasons in influencing the size of oxidation peak current. In addition, it is another reason that the degree of oxygen reduction reaction at auxiliary electrode decreases with the increase of pH. On this basis, it is also proposed about a new point of view that the  $H^+$  gave up in reaction layer for the oxidization of DA, UA and Trp migrates towards cathode along a concentration gradient, which supplements the  $H^+$  consumed in cathode reaction, and at the same time plays two roles: 1) Supplies the energy for the transport of DA, UA and Trp from the diffusion layer to the reaction layer, 2) Promotes the degree of oxidation reaction for DA, UA and Trp at working electrode. Namely,  $i_{p,a}$  of DA, UA and Trp is enlarged along with the  $H^+$  gave up in reaction layer migrating from anode toward cathode. Accordingly, the reason that the size of  $i_{p,a}$  for DA, UA and Trp changes with the pH values can

1  
2  
3 achieve a detailed explanation on the basis of subsequent discussion, and the theoretical  
4 foundation can be provided to select the optimum pH value for electroanalytical experiment.  
5  
6 Therefore, the research was of great theoretical significance and practical value.  
7  
8

## 9 10 **Experimental**

### 11 **Apparatus**

12 All electrochemical experiments were accomplished with CHI832C electrochemical workstation  
13 (Shanghai Chenhua Instrument Company, China) controlled by a microcomputer with CHI 832C  
14 software. A conventional three electrode system was used for all electrochemical experiments,  
15 which comprised of a self-made naked or 316L-PAIUCPE as the working electrode, a platinum  
16 wire as the auxiliary electrode and a saturated calomel electrode (SCE) as the reference electrode.  
17 A PFS-80 digital pH meter (Shanghai Dazhong Analysis Instrument Company, Shanghai, China)  
18 was used for monitor the pH of buffer solution. Ultrasonic cleaning instrument (Kunshan  
19 ultrasonic instrument co., Ltd, Kunshan, China) and Scanning electron microscope (SEM, JEOL  
20 JSM-7500F, Japan) were used.  
21  
22  
23  
24  
25  
26  
27  
28  
29  
30  
31

### 32 **Reagents**

33 All aqueous solutions were prepared with double distilled deionized water and all reagents were of  
34 analytical reagent grade. NaOH(A.R.) and HCl(A.R.) were supplied by Luoyang Haohua Chemical  
35 Reagent Co., Ltd. Luoyang, China. Graphite powder was purchased from Shanghai colloid  
36 chemical plant, Shanghai, China. Paraffin oil was supplied by Xinxiang Henan glass Station.  
37 Henan, China. DA was supplied by Shanghai Hefeng Pharmaceutical Co. Ltd., Shanghai, China.  
38 UA was purchased from Shanghai Chemical Reagent Factory. Shanghai, China. Trp was  
39 purchased from Second Military Medical University from Zhaohui pharmaceutical factory.  
40 Shanghai, China.  $\text{KH}_2\text{PO}_4$ ,  $\text{K}_2\text{HPO}_4$  and  $\text{H}_3\text{PO}_4$  were purchased Beijing Hongxing Chemical Plant.  
41 Beijing, China. Standard solution: Stock solutions of DA ( $4.0 \times 10^{-3}$  mol/L), UA ( $1.0 \times 10^{-2}$  mol/L)  
42 and Trp ( $1.0 \times 10^{-2}$  mol/L) were prepared in water, 0.10 mol/L NaOH, and 0.10 mol/L, respectively,  
43 keeping at 4 °C and avoiding shining or sunlight. The 0.1 mol/L phosphate buffer solutions (PBS)  
44 with various pH values were provided by mixing the stock solutions of 0.10 mol/L  $\text{KH}_2\text{PO}_4$ ,  
45  $\text{K}_2\text{HPO}_4$  and  $\text{H}_3\text{PO}_4$ . Graphite powder and paraffin oil were used as binding agents of the graphite  
46  
47  
48  
49  
50  
51  
52  
53  
54  
55  
56  
57  
58  
59  
60

1  
2  
3 pastes. Urine sample and human serum sample were obtained from The Henan Normal University  
4 Hospital(Provided by volunteers ). All experiments were performed was in compliance with the  
5 Managerial Regulation of the Medical Institutions and IRB guidelines. The informed consent was  
6 obtained for any experimentation with human subjects and Xinxiang City Health Bureau have  
7 approved the experiments.  
8  
9  
10  
11  
12

### 13 14 15 **Preparation of 316L -PAIUCPE**

16 Fully grinded graphite and paraffin oil(4:1, m/m) were mixed and whipped into a smooth paste. A  
17 316L of 2.5 mm in diameter and 5cm in length was sealed in a PTFE tube of 1cm in length, one  
18 end of the rod was used as the electrode connection held out of the plastic tube and the other one  
19 as the working electrode surface. Prior to applied, the electrode surface was polished with alumina  
20 slurry (0.05mm) until a smooth and level surface was obtained, successively washed it with 1:1  
21 nitric acid, absolute ethanol and double distilled water in ultrasonic, and then dried it in the air.  
22 Then the pretreated 316L substrate was rubbed in the carbon paste to fabricate an inlaying  
23 ultrathin carbon paste electrode with 316L as a matrix (316L-IUCPE). The as-prepared  
24 316L-IUCPE was anodized by continuous cyclic voltammograms (CVs) for 30 cycles from 0.0V  
25 to +1.2V with the scan rate of  $100\text{mV}\cdot\text{s}^{-1}$  in NaOH solution ( $0.20\text{mol}\cdot\text{L}^{-1}$ ). After the  
26 pre-anodization, thoroughly rinsed the electrode with double distilled water and dried it at room  
27 temperature, and then 316L-PAIUCPE was obtained.  
28  
29  
30  
31  
32  
33  
34  
35  
36  
37  
38  
39  
40

### 41 **Experimental procedures**

42 A certain volume of DA, UA and Trp standard solution was transferred into a 10mL colorimetric  
43 tube and diluted to degree scale with PBS buffer solution (pH=5.00), then transferred into the  
44 electrochemical cell. The voltammetric behaviors of them were recorded with three electrodes  
45 scanning from 0.00 to +1.20V at a scan rate of  $100\text{mV}\cdot\text{s}^{-1}$  by CVs. After scanning the analytes  
46 each time, the three electrode system were put into the solution of NaOH ( $0.20\text{mol}\cdot\text{L}^{-1}$ ) to update  
47 the surface of working electrode. All experiments were carried out at room temperature.  
48  
49  
50  
51  
52  
53  
54  
55  
56  
57  
58  
59  
60

## Results and discussions

### CVs of $K_4[Fe(CN)_6]$ on different electrodes

-----  
Fig. 1  
-----

$K_4[Fe(CN)_6]$  is commonly used for the investigation of the electrochemical behaviors and properties of the modified electrode. According to the above section 2.4, Fig. 1 depicts the CVs of the naked 316L, 316L-IUCPE and 316L-PAIUCPE in  $K_4[Fe(CN)_6]$  solution ( $1.0 \times 10^{-3} \text{ mol} \cdot \text{L}^{-1}$ ). No oxidation–reduction peaks are found at the naked 316L electrode (Fig. 1a). A pair of broad oxidation-reduction peaks appear at 0.408V and 0.307V on 316L-IUCPE (Fig. 1b). Compared with *curve b*, the redox peaks at 316L-PAIUCPE (Fig. 1c) become sharper and greater, and the interval of peak potentials decrease to 71mV that is closer to the ideal value of 59 mV.<sup>32</sup> Moreover, the ratio of oxidation-reduction peak currents approximately equals to 1, which indicates that a reversible electron transfer process occurs at the 316L-PAIUCPE. This is attributed to the surface of the carbon paste electrode produces abundant active oxygen-containing groups in the process of pre-anodized at 316L-IUCPE surface in  $0.20 \text{ mol} \cdot \text{L}^{-1}$  NaOH solution,<sup>33</sup> which causes the enhancement of local stress, increases the electrode surface area and produces more active sites, therefore, the 316L-PAIUCPE exhibits an excellent electrochemical response. So it is served as working electrode in the experiment.

### The effect of hydrogen catalysis on the CVs of DA, UA and Trp at different electrodes

-----  
Fig. 2  
-----

The amperometric responses of the mixture solution of DA ( $1 \times 10^{-5} \text{ mol} \cdot \text{L}^{-1}$ ), UA ( $1 \times 10^{-5} \text{ mol} \cdot \text{L}^{-1}$ ) and Trp ( $1 \times 10^{-5} \text{ mol} \cdot \text{L}^{-1}$ ) are studied using BR, PBS, acetic acid-sodium acetate and citric

1  
2  
3  
4  
5  
6  
7  
8  
9  
10  
11  
12  
13  
14  
15  
16  
17  
18  
19  
20  
21  
22  
23  
24  
25  
26  
27  
28  
29  
30  
31  
32  
33  
34  
35  
36  
37  
38  
39  
40  
41  
42  
43  
44  
45  
46  
47  
48  
49  
50  
51  
52  
53  
54  
55  
56  
57  
58  
59  
60

acid- $\text{Na}_2\text{HPO}_4$  as the supporting electrolyte separately. The results show that, under the same conditions, maximum peak current and best peak shape of analytes are obtained in PBS buffer solution. The cyclic voltammetric behaviors of DA, UA and Trp are investigated at the scan rate of  $100\text{mV}\cdot\text{s}^{-1}$  in the range of 0.0~1.2V at the 316L-IUCPE, 316L-PAIUCPE. The results are presented in Fig. 2. There is no obvious electrochemical signal for the PBS buffer solution (pH=5.00) without DA, UA and Trp at the 316L-IUCPE(Fig. 2a), which indicates that the determination of analytes can not be interfered by supporting electrolyte. The 316L-IUCPE show a weak electrocatalytic activity(Fig. 2b) toward DA, UA and Trp, and the peak potentials are 0.317V, 0.440V and 0.822V respectively. However, at the 316L-PAIUCPE(Fig. 2c), a dramatically increase of the anodic peak currents is observed, and the corresponding peak potentials are 0.271V, 0.425V and 0.759V separately. According to the principle that the lower the oxidation potential of reducing agents and the easier they to be oxidized, the results reveal that at 316L-PAIUCPE, DA, UA and Trp are easier to loss electrons and are oxidized, which results in that the oxidation peaks of DA, UA and Trp are sharper. The reason can be ascribed to that the activity groups of DA, UA and Trp can interact with negatively-charged oxygen-containing functional groups (ether ( $-\text{O}-$ ), hydroxyl ( $-\text{O}^-$ ), carboxyl ( $-\text{COO}^-$ ), *etc*)<sup>33</sup> at the surface of 316L-PAIUCPE by the hydrogen bonding, thus the adsorption abilities of DA, UA and Trp are enhanced. As shown in Fig. 2, their oxidation peak currents are markedly enlarged due to the formation of hydrogen bonding which is similar to the hydrogen bond catalysis in the organic synthesis<sup>34</sup>. In other words, it is the catalysis that promotes electrochemical oxidations of DA, UA and Trp at the 316L-PAIUCPE. Moreover, the 316L-PAIUCPE surface has more activity groups than the 316L-IUCPE, the formation and catalysis abilities of hydrogen bond are stronger, as a consequence, the oxidation peak currents at 316L-PAIUCPE become greater. Thus, the catalysis of the 316L-PAIUCPE can not only separate oxidation peaks of DA, UA and Trp, but also markedly enlarge the oxidation peak currents.

### The morphology of different electrode surfaces

-----  
Fig. 3  
-----

1  
2  
3  
4  
5  
6  
7  
8  
9  
10  
11  
12  
13  
14  
15  
16  
17  
18  
19  
20  
21  
22  
23  
24  
25  
26  
27  
28  
29  
30  
31  
32  
33  
34  
35  
36  
37  
38  
39  
40  
41  
42  
43  
44  
45  
46  
47  
48  
49  
50  
51  
52  
53  
54  
55  
56  
57  
58  
59  
60

In order to confirm the fabrication procedures, the morphology of the naked 316L, 316L-IUCPE and 316L-PAIUC are characterized by scanning electron microscope (SEM) as shown in Fig. 3. Grooves with several micrometers in width can be estimated on the surface of the bare 316L electrode (Fig. 3a), and its depth is approximately in the range of a few tens of nanometers to several micrometers. It is enough for the inlay of a thin layer of carbon paste, and then an inlaying ultrathin carbon paste electrode is prepared with the naked 316L as the matrix (316L-IUCPE, Fig. 3b). The surface of 316L-IUCPE is flake graphite connected with each other with the thickness of several decades nanometers. After the 316L-IUCPE is pre-anodized, and turn into the pre-anodized 316L-IUCPE (316L-PAIUCPE, Fig. 3c), which possesses a better spatial structure and more intervals among flake graphite and the larger superficial area. Moreover, the hydroxyl group is inlaid into the electrode surface, and many micro-fabricated reactive sites appear.<sup>35</sup> In addition, various oxygen-containing functional groups (ether (–O–), hydroxyl (–OH), carboxyl (–COO<sup>–</sup>), *etc.*) are generated at the electrode surface during the process of its pre-anodization,<sup>33</sup> and the electrocatalytic activity is significantly improved at the same time.

#### Optimization of pre-anodized conditions

The influence of different scan range, cycles of cyclic voltammetry and scan rate on the determination are determined in 0.20 mol·L<sup>–1</sup> H<sub>2</sub>SO<sub>4</sub>, 0.20 mol·L<sup>–1</sup> NaOH and 0.20 mol·L<sup>–1</sup> NaCl solution respectively. The results showed that the best response is obtained when the scan rate is 100 mV·s<sup>–1</sup> with the scan range of 0~1.2 V and CV for 30 cycles in 0.20 mol/L NaOH solution. Therefore, 0.20 mol·L<sup>–1</sup> NaOH is served as pre-oxidized medium.

#### The effect of pH on peak potential

-----  
Fig. 4  
-----

Fig. 4 depicts the impact of pH on oxidation peak potentials, and shows the trend that the peak potential for oxidation of DA, UA and Trp gradually shift negatively as pH increasing, which is

1  
2  
3 almost the same as the phenomenon reported in literature<sup>36</sup>. Good linear relationship is obtained  
4  
5 between  $E_{pa}$  and pH values in the range of pH=2.00~9.00. The linear equations are:  $E_p$  (DA)  
6  
7 =0.5481-0.05488pH(R=0.9991),  $E_p$  (UA) =0.7214-0.05673pH (R=0.9973) and  $E_p$  (Trp)  
8  
9 =1.070-0.04960pH (R=0.9989), respectively. The slopes of equations are close to 59mV/pH,  
10  
11 which illustrates the electrode reactions for oxidation of DA, UA and Trp at the 316L-PAIUCPE  
12  
13 are an equal number of electrons and protons process.  
14  
15

### 16 17 **The effect of pH on peak current of Trp, UA and DA**

#### 18 19 **The effect of pH on peak current of Trp**

20  
21 On the basis of the principia that the lower the oxidation potential of reducing agent and the  
22  
23 stronger the oxidizing its ability, the oxidation peak currents of Trp should be enhanced with the  
24  
25 increase of pH. As a matter of fact, as presented in Fig. 4, the peak current for oxidation of Trp  
26  
27 drops with the rise of pH. The reason may relate to the ionization constant of protonated amidogen  
28  
29 ( $-\text{NH}_3^+$ ) and carboxyl ( $-\text{COOH}$ ) in the molecular structure of Trp. According to  $\text{pK}_{a1}$  (2.35) of the  
30  
31 carboxyl( $-\text{COOH}$ ) and  $\text{pK}_{a2}$  (9.78) of protonated amidogen ( $-\text{NH}_3^+$ ) in glycine molecular, and  
32  
33 assuming the  $\text{pK}_{a1}$ ,  $\text{pK}_{a2}$  of Trp are the same as that of glycin. The greater the acidity, the stronger  
34  
35 the protonation of amidogen( $-\text{NH}_2$ ), leading to the hydrogen bonding or electrostatic force  
36  
37 between the protonated amidogen ( $-\text{NH}_3^+$ ) and 316L-PAIUCPE surface stronger, making the  
38  
39 concentration of Trp at the surface of electrode increase. Therefore, the oxidation peak current is  
40  
41 higher at the greater acidity. However, it is strengthen for deprotonation of protonated amidogen  
42  
43 ( $-\text{NH}_3^+$ ) and ionization degree of carboxyl ( $-\text{COOH}$ ) in the Trp molecular as pH increasing, which  
44  
45 inhibits the hydrogen bonding or electrostatic force between protonated amine group ( $-\text{NH}_3^+$ ) and  
46  
47 the negatively-charged oxygen-containing groups of 316L-PAIUCPE surface. Besides, the  
48  
49 carboxyl anion ( $-\text{COO}^-$ ) ionized by carboxyl ( $-\text{COOH}$ ) of Trp will suffer electrostatic repulsion  
50  
51 from the surface of 316L-PAIUCPE, which causes the concentration of Trp on the electrode  
52  
53 surface decrease with the increase of pH, leading to the oxidation peak current of Trp reduce. Thus,  
54  
55 the size of oxidation peak current for Trp is closely related to different acid-base species for its.  
56  
57 The protonated Trp ( $\text{RCH}(\text{NH}_3^+)\text{CH}_2\text{COOH}$ ), the dipole ion ( $\text{RCH}(\text{NH}_3^+)\text{CH}_2\text{COO}^-$ ) and anion  
58  
59 ( $\text{RCH}(\text{NH}_2)\text{CH}_2\text{COO}^-$ ) of Trp are expressed as  $^+\text{H}_2\text{A}$ ,  $^+\text{HA}^-$  and  $\text{A}^-$ , respectively. The distribution  
60

1  
2  
3 fractions of the  ${}^+H_2A$ ,  ${}^+HA^-$  and  $A^-$  respectively account for 69.1%, 31.9%, 0.0% at pH=2.0 and  
4  
5 0.0%, 91%, 9% at pH=9.0, the oxidation peak current of Trp reduce from 3.35 $\mu$ A to 0.95 $\mu$ A.  
6  
7 Consequently, the oxidation peak current of Trp reduces with the decrement of  ${}^+H_2A$  and the  
8  
9 increments of  ${}^+HA^-$  and  $A^-$ . The reasons may be as follows: 1) The amounts of Trp with  
10  
11 negatively-charged carboxyl anion ( $-COO^-$ ) increase with the increment of pH value, 2) Under the  
12  
13 conditions of larger pH value, the carboxyl ( $-COOH$ ) at the surface of 316L- PAIUCPE will be  
14  
15 ionized into carboxyl anion( $-COO^-$ ), 3) Based on the above two points, with the increment of pH  
16  
17 value, it is greatly weakened to the interaction of oxygen-containing functional groups at the  
18  
19 surface of 316L- PAIUCPE with the amidogen ( $-NH_2$ ) and carboxyl ( $-COOH$ ) of Trp by the  
20  
21 hydrogen bond, so do the hydrogen bond catalysis.  
22  
23

#### 24 The effect of pH on peak current of UA

25  
26  
27 -----  
28

29 Fig. 5  
30  
31 -----  
32

33 Similarly, on the basis of discussion in section 3.6.1, the oxidation potential of UA decrease with  
34  
35 the raise of pH, the more highly oxidized the reduced form UA should be. However, as depicted in  
36  
37 Fig. 4, the oxidation peak current of UA dropped with the rise of pH in the range of pH =2.00-5.00.  
38  
39 In the range of pH =5.00-6.00, the peak current remains unchanged. While pH value exceeds 6.00,  
40  
41  $i_{pa,UA}$  decrease continuously with the increase of pH.  
42

43 In order to explain this phenomenon, take 8-hydroxyl UA<sup>37</sup> as an example to examine the  
44  
45 effect of the acidity on the size of  $i_{pa,UA}$ . When the acidity of solution is high, assuming N<sub>7</sub> in the  
46  
47 isomer of 8-hydroxyl UA can be protonated as similar as N<sub>7</sub> (pK<sub>a1</sub>=2.3) of G,<sup>38</sup> accordingly, the  
48  
49 numerical value of dissociation constant (pK<sub>a1</sub>) of the protonated N<sub>7</sub> for UA ought to be similar to  
50  
51 that of G (see Fig. 5).  
52

53 In our case, as the N<sub>7</sub> in the 8-hydroxyl UA can be protonated under the higher acidity  
54  
55 condition, and the positively-charged protonated N<sub>7</sub> (as shown in Fig. 5) can be also intensely  
56  
57 attracted by negatively-charged oxygen-containing functional groups ( $-O^-$ ,  $-COO^-$ , *etc.*) on the  
58  
59 316L- PAIUCPE surface. Thus, the total amounts of UA diffusing to the reaction layer increase  
60

1  
2  
3  
4  
5  
6  
7  
8  
9  
10  
11  
12  
13  
14  
15  
16  
17  
18  
19  
20  
21  
22  
23  
24  
25  
26  
27  
28  
29  
30  
31  
32  
33  
34  
35  
36  
37  
38  
39  
40  
41  
42  
43  
44  
45  
46  
47  
48  
49  
50  
51  
52  
53  
54  
55  
56  
57  
58  
59  
60

with the enhancement of the solution acidity. In addition, owing to the protonated N<sub>7</sub> interacts with active groups, the oxidized C<sub>8</sub> in UA also approach the surface of 316L- PAIUCPE by hydrogen bonding. As a result, the peak current of UA has a greater value under the higher acidity condition. In contrast, when pH value increases from 2.0 to 5.0,  $i_{pa,UA}$  decreases from 3.23 $\mu$ A to 1.67 $\mu$ A, accordingly, which results from that the deprotonation of the protonated UA (H<sub>2</sub>UA<sup>+</sup>) enlarges with the rise of pH in feed solution. Therefore, the amounts of UA diffuse to the reaction layer diminish with the increment of pH, which makes the  $i_{pa,UA}$  decrease. Based on the discussions above, in the light of the (pK<sub>a2</sub>=5.4) hydroxyl of UA,<sup>39</sup> supposing the dissociation constant (pK<sub>a1</sub>) of the protonated N<sub>7</sub> of 8-hydroxyl UA is the same as that of the protonated N<sub>7</sub> (pK<sub>a1</sub>=2.3) of G, it can be calculated that the H<sub>2</sub>UA<sup>+</sup>, neutral molecules (HUA) in the solution separately account for 17 per cent and 83 per cent of UA at pH=3.00 on the basis of the distribution fractions of UA in different species. At pH=5.00, HUA and monovalent anion (UA<sup>-</sup>) account for 71 per cent and 29 per cent of UA, by the deprotonation of H<sub>2</sub>UA<sup>+</sup>. It will be seen from this that the size of peak current for oxidation of UA should be closely related to the amounts of the different acid-base species. Although the higher oxidation peak potential of UA under the higher acidity condition, the higher acidity of solution lead to larger amount of H<sub>2</sub>UA<sup>+</sup> in the solution and finally a greater oxidation peak current of UA is obtained.

The amounts of UA<sup>-</sup> ionized by HUA increase with the rise of pH, HUA and UA<sup>-</sup> account for 20 per cent and 80 per cent of UA respectively at pH=6.00. Compared with pH=5.00, the percentage of UA<sup>-</sup> has a increase of 51 per cent, which may result in the amounts of UA that diffuse to the reaction layer dramatically diminish. However, the  $i_{pa,UA}$  has only a tiny change from 1.67 $\mu$ A to 1.63 $\mu$ A in the range of pH= 5.00-6.00. But when pH > 6.00,  $i_{pa,UA}$  decreases continuously with the increment of pH. The reason is that with the increase of pH, more and more HUA can be ionized into UA<sup>-</sup> repelled by the negatively-charged 316L-PAIUCPE surface in the anode reaction layer. Therefore, the amounts of UA diffusing to the reaction layer are diminished, and then the peak current for oxidation of UA decreases with the increment of pH accordingly. In conclusion, besides the oxidation peak potential, the size of peak current for oxidation of UA should has a close relationship with the distribution fractions of the different acid-base species for UA. Moreover, the stronger the interaction between the different acid-base species of UA and electrode surface, the greater the hydrogen bond catalysis and the greater the oxidation peak

1  
2  
3  
4  
5  
6  
7  
8  
9  
10  
11  
12  
13  
14  
15  
16  
17  
18  
19  
20  
21  
22  
23  
24  
25  
26  
27  
28  
29  
30  
31  
32  
33  
34  
35  
36  
37  
38  
39  
40  
41  
42  
43  
44  
45  
46  
47  
48  
49  
50  
51  
52  
53  
54  
55  
56  
57  
58  
59  
60

current.

### The effect of pH on peak current of DA

Contrary to UA and Trp, a increase of oxidation peak current for DA is observed as the pH of solution increases from 2.00 to 7.00. When pH exceeds 7.00,  $i_{pa,DA}$  decreases with the increment of pH. The reason may be that the size of  $i_{pa,DA}$  is also related to molecular configuration of DA. The two phenolic hydroxyls in the molecular structure of DA are similar to o-dihydroxybenzene, whose  $pK_{a1}$ ,  $pK_{a2}$  should be close or identical that of o-dihydroxybenzene, they are respectively 9.44 and 12.8. And the ethylamino in DA can be also protonated, and the dissociation constant ( $pK_a$ ) of the protonated ethylamino should be similar to that ( $pK_a = 10.75$ ) of the protonated ethylamine (see Fig. 5). Therefore, we assume in our discussions that the  $pK_a$  of the protonated ethylamino is equal to 10.75, and the higher the acidity of solution, the stronger the protonation of ethylamino for DA. According to the dissociation constants ( $pK_{a1}=9.44$ ,  $pK_{a2}=12.8$ ,  $pK_a=10.75$ ) of DA ( $H_3DA^+$ ) mentioned above (Fig. 5), it can be calculated that the protonated DA ( $H_3DA^+$ ) account for 100 per cent of DA at  $pH=2.00$ , and the amounts of its neutral molecules is equal to zero. Due to the low steric effects, the positively-charged protonated ethylamino in the reaction layer should be preferentially attracted by the negatively-charged oxygen-containing functional groups at the 316L-PAIUCPE surface, which induces the phenolic hydroxyls in DA which can take part in electrode reaction are far away from the 316L- PAIUCPE surface. Therefore, in strong acidity condition,  $E_{pa,DA}$  is higher and the phenolic hydroxyl is not easy to be oxidized, leading to the  $i_{pa,DA}$  is lower. In the pH range of 2.00 to 7.00,  $i_{pa,DA}$  enhances with the increment of pH and arrives its maximum at  $pH=7.0$ . This phenomenon can be attributed to the following three reasons: with the increment of pH, 1) the degree of the deprotonation for the protonated DA enlarges, which is more beneficial to making the phenolic hydroxyls in DA expose to the electrode surface for further oxidized, 2) the amounts of negatively-charged carboxyl anion ( $-COO^-$ ) ionized by the carboxyls ( $-COOH$ ) at the 316L-PAIUCPE surface increase, which enhances the formation of hydrogen bonds between phenolic hydroxyl in DA and the carboxyl anion ( $-COO^-$ ) as well as hydrogen bond catalysis, 3) the oxidation peak potential of DA shifts negatively.

When  $pH>7.00$ ,  $i_{pa,DA}$  decreases with the increase of pH. One of the reasons may be that the amounts of phenolic hydroxyl anion ( $-O^-$ ) ionized by the phenolic hydroxyl ( $-OH$ ) will

1  
2  
3 dramatically increase, which diminishes concentration of DA at the 316L-PAIUCPE surface due to  
4 the electrostatic repulsion, resulting in peak current of DA reduces with the increase of pH at  
5 pH>7.00. This shows that the size of oxidation peak current of DA is not only related to its  
6 concentration diffusion but also closely related to the distribution fractions of different acid-base  
7 species for it.  
8  
9  
10  
11  
12

### 13 14 15 **The effect of the degree of reduction reaction at the auxiliary electrode on the oxidation peak** 16 **current of Trp, UA and DA** 17

18 As recorded in Fig. 4, the oxidation peak potentials of Trp, UA and DA always shift negatively  
19 with the rise of pH. The more negative the electrode potential, the greater the tendency of the  
20 reduced form to be oxidized should be. In fact, the oxidation peak currents of them all evidently  
21 decrease with increment of pH at pH>7.0. How to explain the phenomenon has not been reported  
22 in current literature. In our opinion, in addition to the above reasons (3.6.1, 3.6.2 and 3.6.3),  
23 another reason may be that the decrement of degree of auxiliary electrode reaction induces a  
24 decrease of the oxidation peak current of Trp, UA and DA with increment of pH.  
25  
26  
27  
28  
29  
30  
31

### 32 **The effects of acidic solution on the degree of reduction reaction at the auxiliary electrode**

33 Trp, UA and DA are oxidized at the working electrode (316L-PAIUCPE), there must be an  
34 electroactive species is reduced at the auxiliary electrode correspondingly, and the active species  
35 may be H<sup>+</sup> or oxygen dissolved in feed solution. But, the over-potential of hydrogen on the  
36 auxiliary electrode (Pt) is too high, which makes H<sup>+</sup> hardly be reduced at its surface. Hence, the  
37 target that can be reduced is only oxygen. According to Trp, UA and DA that lost two electrons to  
38 be oxidized at the working electrode and oxygen is reduced at the auxiliary electrode, it seems  
39 reasonable that the mechanism of anode-cathode reaction(Scheme.1).  
40  
41  
42  
43  
44  
45  
46

47 -----

48 Scheme.1

49 -----  
50  
51

52 It is evident that the H<sup>+</sup> which released in reaction layer due to the oxidization of Trp, UA and  
53 DA can migrate to cathode along a concentration gradient to supplement the H<sup>+</sup> consumed by the  
54 oxygen reduction reaction at the auxiliary (cathode) electrode, this supplies the energy for the  
55 transport of them from the diffusion layer to the reaction layer. Moreover, the lower the pH value,  
56  
57  
58  
59  
60

1  
2  
3 the greater the tendency of oxygen to be reduced. Based on the principle of equal numbers of  
4 electron gain and loss in the oxidation–reduction reactions, the amounts of Trp, UA and DA to be  
5 oxidized at the anode should be increased with increment of degree of reduction reaction for  
6 oxygen. But, except DA, the larger oxidation peak currents of Trp and UA are obtained under the  
7 condition of lower pH values. The reason why  $i_{pa,DA}$  become lower in the higher acidity is that the  
8 protonated ethylamino with positively-charged DA is preferentially attracted by the 316L-  
9 PAIUCPE surface.  
10  
11

### 12 **The effects of alkaline solution on the degree of reduction reaction at the auxiliary electrode**

13 As shown in“Scheme. 1”, in the alkaline solution, the  $H^+$  given up by the Trp, UA and DA to be  
14 oxidized can be directly neutralized by  $OH^-$  in feed solution, so that the  $H^+$  consumed by the  
15 oxygen reduction reaction can not be effectively supplemented, which results in the reduction  
16 reaction degree of oxygen decreases with the increment of pH. In a conclusion, even if the abilities  
17 of Trp, UA and DA to be oxidized are enlarged in the alkaline solution, their oxidation peak  
18 currents will still decrease due to the decrease of reduction reaction degree for oxygen. The  
19 conclusion is the decrement of degree of the oxygen reduction reaction obviously induce the  
20 decreases of oxidation peak currents for Trp, UA and DA with the increase of pH at pH > 7.0 (see  
21 Fig. 4).  
22  
23

24 For the reasons given above, it can be concluded that the size of  $i_{pa}$  not only closely relate to  
25 pH values of the solution, diffusion behaviors of Trp, UA and DA with different species, the  
26 formation and catalysis of hydrogen bond, molecular configuration mentioned above, but also  
27 relate to the degree of the reduction reaction for oxygen at the cathode.  
28  
29

### 30 **The impact of scan rate**

31 The effect of different scan rate on oxidation peak currents of DA( $8.0 \times 10^{-6} \text{ mol} \cdot \text{L}^{-1}$ ), UA( $1.0 \times 10^{-5}$   
32  $\text{mol} \cdot \text{L}^{-1}$ ) and Trp( $1.0 \times 10^{-5} \text{ mol} \cdot \text{L}^{-1}$ ) is studied by cyclic voltammetry. It is found that the oxidation  
33 peak current increased linearly with the square root of the scan rate( $V^{1/2}$ ) in the range of  
34 0.02~0.35V·s<sup>-1</sup>. The linear equations are  $I_p(\text{DA}) = -0.355 + 0.131 V^{1/2}$  (R=0.9954),  $I_p(\text{UA})$   
35  $= -0.491 + 0.214 V^{1/2}$  (R=0.9969) and  $I_p(\text{Trp}) = -0.600 + 0.230 V^{1/2}$  (R=0.9948) and conform to the  
36 Randles-Sevcik equation [22], which indicates that the oxidation reaction process of DA, UA and  
37  
38  
39  
40  
41  
42  
43  
44  
45  
46  
47  
48  
49  
50  
51  
52  
53  
54  
55  
56  
57  
58  
59  
60

Trp on the working electrode is a diffusion controlled process. In order to ensure a greater peak current and a better peak shape,  $100 \text{ mV} \cdot \text{s}^{-1}$  is selected for the entire experiment.

### The influence of initial potential

Fix the mixture concentration of DA ( $8.0 \times 10^{-6} \text{ mol} \cdot \text{L}^{-1}$ ), UA ( $1.0 \times 10^{-5} \text{ mol} \cdot \text{L}^{-1}$ ) and Trp ( $1.0 \times 10^{-5} \text{ mol} \cdot \text{L}^{-1}$ ) and change the initial potential in the range of  $-0.3 \sim 0.1 \text{ V}$ , the result shows that the peak current increases with the initial potential shifted negatively, when the initial potential was  $0.0 \text{ V}$ , the peak current and baseline are relatively stable, so  $0.0 \text{ V}$  is selected in the experiment as the best initial potential.

### Calibration curve and detection limit

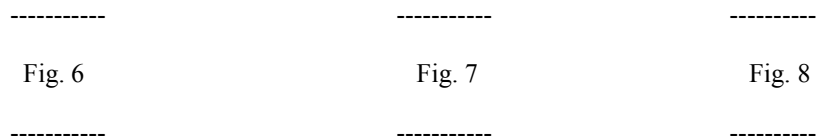


Fig. 6-8 illustrates the electrochemical behavior of DA, UA and Trp in PBS buffer solution ( $\text{pH}=5.00$ ) at 316L-PAIUCPE. The results show that the oxidation peak current of  $I_p$  (DA),  $I_p$  (UA) and  $I_p$  (Trp) increase proportionally with their concentrations in the range of  $0.4 \sim 200.0 \mu\text{mol} \cdot \text{L}^{-1}$ ,  $0.5 \sim 150 \mu\text{mol} \cdot \text{L}^{-1}$  and  $0.1 \sim 200 \mu\text{mol} \cdot \text{L}^{-1}$  respectively. The linear equations are  $I_{p(\text{DA})} (\mu\text{A}) = 0.441 + 0.070c (\mu\text{mol} \cdot \text{L}^{-1})$  ( $R=0.9971$ ),  $I_{p(\text{UA})} (\mu\text{A}) = 0.068 + 0.108c (\mu\text{mol} \cdot \text{L}^{-1})$  ( $R=0.9998$ ) and  $I_{p(\text{Trp})} (\mu\text{A}) = 0.703 + 0.094c (\mu\text{mol} \cdot \text{L}^{-1})$  ( $R=0.9969$ ) respectively. Parallel determination of 11 reagent blank solution could calculate that the detection limit ( $3S/K$ ) of DA, UA and Trp are  $6.8 \times 10^{-8} \text{ mol} \cdot \text{L}^{-1}$ ,  $4.5 \times 10^{-8} \text{ mol} \cdot \text{L}^{-1}$  and  $5.3 \times 10^{-8} \text{ mol} \cdot \text{L}^{-1}$  respectively.

### The stability and reproducibility of 316L-PAIUCPE

In order to test the reproducibility and stability of the working electrode, repetitive measurements are made for the mixtures of DA ( $1.0 \times 10^{-5} \text{ mol} \cdot \text{L}^{-1}$ ), UA ( $1.0 \times 10^{-5} \text{ mol} \cdot \text{L}^{-1}$ ) and Trp ( $1.0 \times 10^{-5} \text{ mol} \cdot \text{L}^{-1}$ ). The relative standard deviations of oxidation peak currents for them are 4.1%,

3.5% and 3.7% (n=11), respectively. The results reveal that the 316L-PAIUCPE has better reproducibility. After the 316L-PAIUCPE is stored for 7 days at room temperature, their oxidation peak current decrease or increase less than 5% of the initial signal, which indicates a long-term stability for the 316L-PAIUCPE.

### Interference of coexisting components

For evaluating selectivity of 316L-PAIUCPE, according to the test method of 2.4, various possible interfering species are examined for their effects on the determination of DA, UA and Trp. The tolerable limit of the foreign substance is defined as the deviations produced by them below 5%. Results show that 500 times of  $K^+$ ,  $NH_4^+$ ,  $Na^+$ ,  $NO_3^-$ ,  $SO_4^{2-}$ ,  $CL^-$ , 300 times of  $Ca^{2+}$ ,  $AL^{3+}$ , 20 times of glycine, L-cysteine does not influence the determination of DA, that 800 times of  $NH_4^+$ ,  $K^+$ ,  $Na^+$ ,  $NO_3^-$ ,  $CL^-$ , 400 times  $Ca^{2+}$ ,  $SO_4^{2-}$ , 100 times of glycine, 2 times L-cysteine does not interference the determination of UA, that 1000 times of  $K^+$ ,  $NH_4^+$ ,  $Na^+$ ,  $SO_4^{2-}$ ,  $CL^-$ ,  $Ca^{2+}$ , 200 times of  $NO_3^-$ , 20 times of  $AL^{3+}$ , 10 times of glycine, L-cysteine does not affect determination of Trp. But epinephrine, norepinephrine, ascorbic acid, isoproterenol, levodopa show interference in the determination of DA, carbidopa show interference in the determination of UA. Although ascorbic acid show interference, this interference could be minimized, if necessary, by using ascorbic oxidase enzyme, which exhibits a high selectivity to the oxidation of ascorbic acid.

### Analytical application

Take DA hydrochloride injection (2ml:20mg) 1ml, the healthy adult fresh urine(centrifugal treatment) 10mL and fresh serum 5mL from the hospital of Henan Normal University, then dilute to 100mL with PBS buffer solution(pH=5.00) respectively and shake well. According to the experimental method of 2.4, the contents of DA, UA and Try are detected by standard addition method. The results are showed in Table1. The recovery rates of DA, UA and Trp are 99.2%~103.8%, 99.7%~101.5% and 99.6%~101.8%, respectively.

-----  
Table.1

## Conclusions

In this paper, 316L-PAIUCPE is constructed on the basis of 316L stainless steel of industrial leftover, and the behaviors of electrochemical response for DA, UA and Trp are researched using it as working electrode. And the influencing mechanisms of acidity on the size of the oxidation peak currents ( $i_p$ ) for DA, UA and Trp are discussed in detail. This method presented is successfully applied for determination of DA, UA, Trp in different samples.

## Acknowledgments

The authors thank the financial supports from the Joint Funds of the Natural Science Foundation of China (No. U1304211), Henan Education Bureau Foundation of China (Nos.13A150507 and 13A150512), Henan Provincial Department of Science and Technology Foundation of China (Nos.132300410294 and 132300410299) and Henan Key Science and Technology Program of China (No. 132102210256).

## References

1. Z.H. Wang, D. Wang, *Chin. J. Anal. Lab.*, 2005, **24**, 43-46.
2. A.E. Radi, H.M. Nassef, A. El-Basiony, *Dyes Pigments*, 2013, **99**, 924-929.
3. J.F. Huang, H.H. Chen, *Talanta*, 2013, **116**, 852-859.
4. G.G. Oliveira, D.C. Azzi, F.C. Vicentini, *J. Electroanal. Chem.*, 2013, **708**, 73-79.
5. H. Beitollahi, I. Sheikhshoaie. *Electrochim. Acta*, 2011, **56**, 10259-10263.
6. H. Beitollahi, I. Sheikhshoaie. *Anal. Methods*, 2011, **3**, 1810-1814.
7. E. Molaakbari, A. Mostafavi, H. Beitollahi, R. Alizadeh. *Analyst*, 2014, **139**, 4356-4364.
8. H. Beitollahi, I. Sheikhshoaie. *J. Electroanal.chem.*, 2011, **661**, 336-342.
9. Hadi Beitollahi, R. Jahan-Bakhsh, R. Hosseinzadeh. *Talanta*, 2011, **85**, 2128-2134.
10. H. Beitollahi, A. Mohadesi, S. Mohammadi, A. Akbari. *Electrochim. Acta*, 2012, **68**, 220-226.
11. H. Beitollahi, M. Mostafavi. *Electroanal*, 2014, **26**, 1090-1098.
12. E.Y.Z. Frag, M.A. Zayed, M.M. Omar, S.E.A. Elashery, G.G. Mohamed, *Int. J. Electrochem. Sci.*, 2012, **7**, 650-662.
13. H.S. El-Desoky, M.M. Ghoneim, *Talanta*, 2011, **84**, 223-234.
14. G.Y. Xu, F.P. Wang, L.N. Tang, *Chem. Res.*, 2008, **19**, 108-112.

- 1  
2  
3  
4 15. Z.H. Wang, Z.J. Zhao, L.L. Zhang, F.J. Zhao, G.Q. Guo, S.P. Zhou, *Acta Chim. Sinica*, 2004,  
5  
6 **62**, 1237-1241.  
7  
8  
9 16. T.P. Singh, H. Singh, H. Singh, *J. Therm. Spray Technol.*, 2012, **21**, 917-927.  
10  
11 17. E.D.L. Heras, D.A. Egidi, P. Corengia, D. González-Santamaría, A. García-Luis, M. Brizuela,  
12  
13 G.A. López, M. Flores Martinez, *Surf. Coat. Technol.*, 2008, **202**, 2945-2954.  
14  
15  
16 18. J. Pellier, J. Geringer, B. Forest, *Wear*, 2011, **271**, 1563-1571.  
17  
18  
19 19. L. Yang, D.W. Wang, J.S. Huang, *Electrochem. Commun.*, 2010, **12**, 1108-1111.  
20  
21 20. A. Safavi, N. Maleki, F.A. Mahyari, *Fullerenes Nano. Carb. Nanostruct.*, 2013, **21**, 472-484.  
22  
23 21. F. Valentini, D. Romanazzo, M. Carbone, *Electroanal.*, 2012, **24**, 872-881.  
24  
25  
26 22. F. Valentini, S. Orlanducci, E. Tamburri, M.L. Terranova, *Electroanal.*, 2005, **17**, 28-37.  
27  
28  
29 23. L.M. Niu, K.Q. Lian, H.M. Shi, *Sens. Actuators, B*, 2013, **178**, 10-18.  
30  
31 24. T. Tavana, M.A. Khalilzadeh, H. Karimi-Maleh, A.A. Ensafi, H. Beitollahi, D. Zareyee, *J. Mol.*  
32  
33 *Liq.*, 2012, **168**, 69-74.  
34  
35  
36 25. T. Thomas, R.J. Mascarenhas, P. Martis, Z. Mekhalif, B.E. Kumara Swamy, *Mater. Sci. Eng.,*  
37  
38 *C*, 2013, **33**, 3294-3302.  
39  
40  
41 26. Y.H. Zeng, J.Q. Yang, K.B. Wu, *Electrochim. Acta*, 2008, **53**, 4615-4620.  
42  
43  
44 27. S. Shahrokhian, M. Ghalkhani, M.K. Amini, *Sens. Actuators, B*, 2009, **137**, 669-675.  
45  
46  
47 28. S. Chitravathi, B.E. Kumara Swamy, G.P. Mamatha, B.S. Sherigara, *J. Mol. Liq.*, 2011, **160**,  
48  
49 193-199.  
50  
51  
52 29. N.F. Atta, A. Galal, R.A. Ahmed, *Bioelectrochem.*, 2011, **80**, 132-141.  
53  
54  
55 30. M. Amiri, A. Bezaatpour, Z. Pakdel, K. Nekoueian, *J. Solid State Electrochem.*, 2012, **16**,  
56  
57 2187-2195.  
58  
59  
60

- 1  
2  
3  
4 31. O.J. D'Souza, R.J. Mascarenhas, T. Thomas, I.N.N. Namboothiri, M. Rajamathi, P. Martis, J.  
5  
6 Dalhalle, *J. Electroanal. Chem.*, 2013, **704**, 220-226.  
7  
8  
9 32. A.J. Bard, L.R. Faulkner, *Electrochem. Methods: Fundam. Appl.*, second ed., 2001, John  
10  
11 Wiley&Sons Inc., New York, 856.  
12  
13 33. H.C. Zhang, X.B. Zuo, M.R. Ji, *Acta Phys., Chim. Sinica*, 1996, **12**, 649-653.  
14  
15 34. X.H. Yu, W. Wang, *Chem. Asian J.*, 2008, **3**, 516-532.  
16  
17 35. R.L. McCreery, *Chem. Rev.*, 2008, **108**, 2646-2687.  
18  
19 36. Z.H. Guo, S.J. Dong, *Electroanal.*, 2005, **17**, 607-612.  
20  
21 37. W.K. Chen, C.H. Lu, J. Xu, *Chin. J. Struct. Chem.*, 2002, **21**, 186-190.  
22  
23 38. D.W. Yu, J.N. Zhu, W.Z. Ke, *Spectrosc. Spec. Anal.*, 2003, **23**, 734-738.  
24  
25 39. J. Li, X.Q. Lin, *Anal. Chim. Acta*, 2007, **596**, 222-230.  
26  
27  
28  
29  
30  
31  
32  
33  
34  
35  
36  
37  
38  
39  
40  
41  
42  
43  
44  
45  
46  
47  
48  
49  
50  
51  
52  
53  
54  
55  
56  
57  
58  
59  
60

1  
2  
3  
4  
5  
6 **The effect of acidity, hydrogen bond catalysis and auxiliary electrode**  
7  
8 **reaction on the oxidation peak current for dopamine, uric acid and**  
9  
10 **tryptophan**

11  
12 Yixuan Li, Jing Li, Enbo Shangguan\* and Quanmin Li\*  
13 (School of Chemistry and Chemical Engineering, Henan Normal University,  
14 Xixiang, Henan, 453007, P.R. China)  
15  
16  
17  
18  
19  
20  
21  
22  
23  
24

25 **Figure Legends**

26  
27  
28 **Fig.1 CVs of  $K_4[Fe(CN)_6]$  on different electrodes**

29 a. naked 316L; b. 316L-IUCPE; c. 316L-PAIUCPE;  $c(K_4[Fe(CN)_6]): 1.0 \times 10^{-3} \text{ mol} \cdot \text{L}^{-1}$ ;  
30 Scan rate:  $0.1 \text{ V} \cdot \text{s}^{-1}$ ; Supporting electrolyte:  $0.10 \text{ mol} \cdot \text{L}^{-1} \text{H}_2\text{SO}_4$   
31  
32  
33  
34

35  
36 **Fig.2 CVs of DA, UA and Trp on different electrodes**

37 a: 316L-PAIUCPE in PBS(pH=5.00) without DA, UA and Trp ; b: 316L-IUCPE ; c:  
38 316L-PAIUCPE; Scan rate:  $0.1 \text{ V} \cdot \text{s}^{-1}$ ; Supporting electrolyte: PBS(pH=5.00);  
39 1.  $c(\text{DA}): 1.0 \times 10^{-5} \text{ mol} \cdot \text{L}^{-1}$ ,  
40 2.  $c(\text{UA}): 1.0 \times 10^{-5} \text{ mol} \cdot \text{L}^{-1}$ , 3.  $c(\text{Trp}): 1.0 \times 10^{-5} \text{ mol} \cdot \text{L}^{-1}$ .  
41  
42  
43  
44  
45  
46

47 **Fig.3 SEMs of different electrode surfaces**

48 a: 316L; b: 316L-IUCPE; c: 316L-PAIUCPE  
49  
50  
51

52 **Fig.4 Effect of pH on  $E$  and  $I$**

53  $c(\text{DA}): 4.0 \times 10^{-5} \text{ mol} \cdot \text{L}^{-1}$ ,  $c(\text{UA}): 2.0 \times 10^{-5} \text{ mol} \cdot \text{L}^{-1}$ ,  $c(\text{Trp}): 2.0 \times 10^{-5} \text{ mol} \cdot \text{L}^{-1}$ . Supporting  
54  
55  
56

57 \* Corresponding author. Tel.: +86 373 3326336; fax: +86 373 3326336.  
58 E-mail address: shangguanbo@163.com (E. Shangguan) ; mercury6068@hotmail.com (Q.Li)  
59  
60

1  
2  
3 electrolyte:PBS (pH=2.00~9.00), scan rate:  $0.1\text{V}\cdot\text{s}^{-1}$ .  
4  
5  
6

7 **Fig.5 The protonation of different molecules**  
8  
9

10 **Fig.6 LSVs for the determination of DA**

11 a→k:c(DA)=0.4, 1, 4, 8, 16, 28, 36, 40, 60, 80, 120, 160, 200 $\mu\text{mol}\cdot\text{L}^{-1}$ ,  
12 c(UA)= $3.0\times 10^{-6}\text{mol}\cdot\text{L}^{-1}$ , c(Trp)= $2.0\times 10^{-6}\text{mol}\cdot\text{L}^{-1}$ . Supporting electrolyte:0.1M  
13 PBS(pH=5.00), scan rate:  $0.1\text{V}\cdot\text{s}^{-1}$ .  
14  
15  
16  
17  
18  
19

20 **Fig.7 LSVs for the determination of UA**

21 a→l:c(AC)=0.5, 1, 3, 5, 7, 10, 20, 40, 60, 80, 100, 150  $\mu\text{mol}\cdot\text{L}^{-1}$ ,  
22 c(DA)= $1.0\times 10^{-5}\text{mol}\cdot\text{L}^{-1}$ , c(Trp)= $5.0\times 10^{-6}\text{mol}\cdot\text{L}^{-1}$ . Supporting electrolyte: 0.1 $\text{mol}\cdot\text{L}^{-1}$   
23 PBS(pH=5.00), scan rate:  $0.1\text{V}\cdot\text{s}^{-1}$ .  
24  
25  
26  
27  
28  
29

30 **Fig.8 LSVs for the determination of Trp**

31 a→p:c(Trp)=0.1, 0.5, 1, 3, 5, 7, 10, 20, 40, 50, 60, 70, 80, 100, 150, 200  $\mu\text{mol}\cdot\text{L}^{-1}$ ,  
32 c(DA)= $4.0\times 10^{-6}\text{mol}\cdot\text{L}^{-1}$ , c(UA)= $3.0\times 10^{-6}\text{mol}\cdot\text{L}^{-1}$ . Supporting electrolyte: 0.1M PBS  
33 (pH=5.00), scan rate:  $0.1\text{V}\cdot\text{s}^{-1}$ .  
34  
35  
36  
37  
38  
39  
40  
41  
42  
43  
44  
45  
46  
47  
48  
49  
50  
51  
52  
53  
54  
55  
56  
57  
58  
59  
60

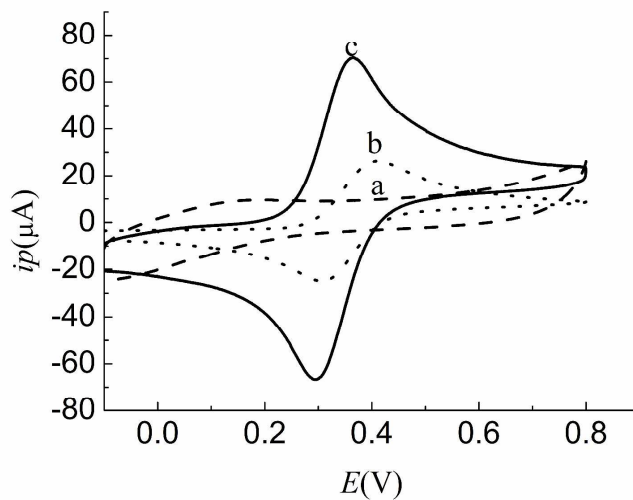


**Fig.1** CVs of  $K_4[Fe(CN)_6]$  on different electrodes

**Fig.1**

1  
2  
3  
4  
5  
6  
7  
8  
9  
10  
11  
12  
13  
14  
15  
16  
17  
18  
19  
20  
21  
22  
23  
24  
25  
26  
27  
28  
29  
30  
31  
32  
33  
34  
35  
36  
37  
38  
39  
40  
41  
42  
43  
44  
45  
46  
47  
48  
49  
50  
51  
52  
53  
54  
55  
56  
57  
58  
59  
60

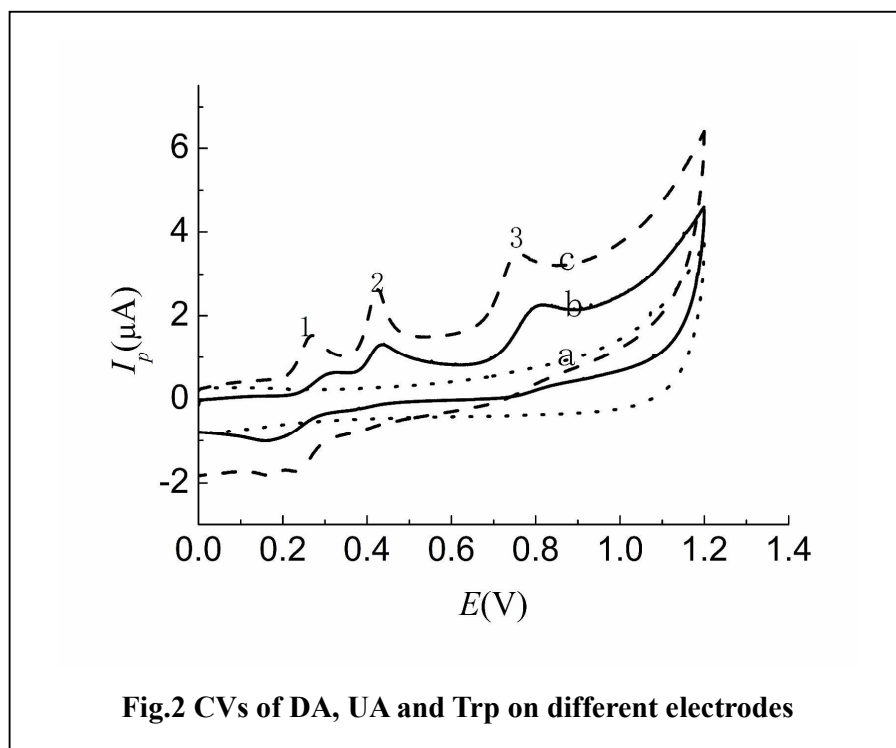
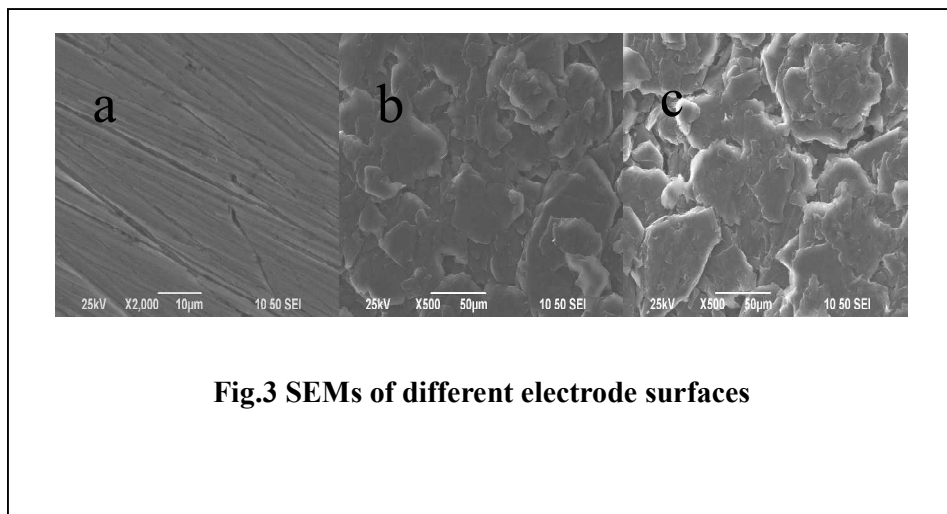


Fig. 2

1  
2  
3  
4  
5  
6  
7  
8  
9  
10  
11  
12  
13  
14  
15  
16  
17  
18  
19  
20  
21  
22  
23  
24  
25  
26  
27  
28  
29  
30  
31  
32  
33  
34  
35  
36  
37  
38  
39  
40  
41  
42  
43  
44  
45  
46  
47  
48  
49  
50  
51  
52  
53  
54  
55  
56  
57  
58  
59  
60



**Fig. 3**

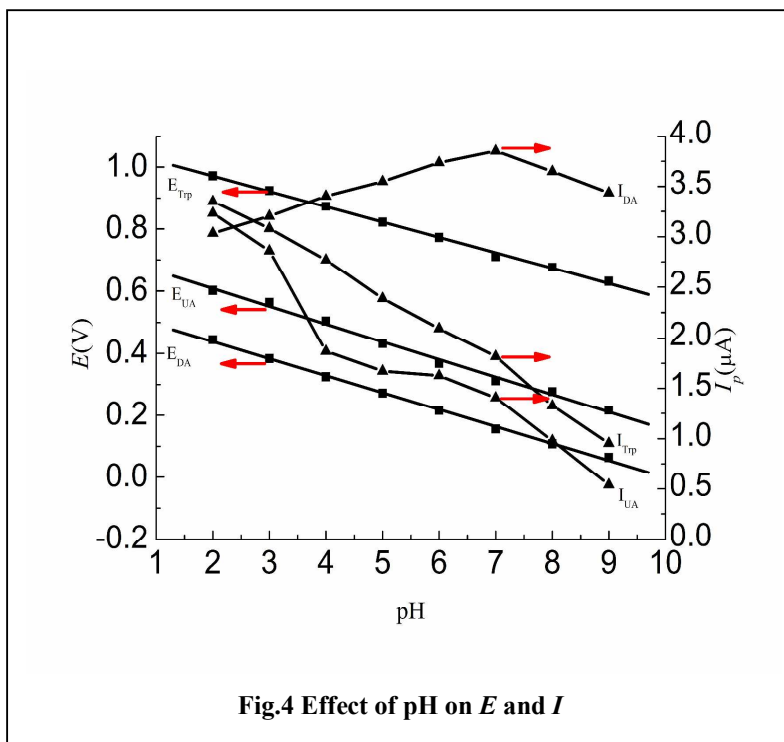


Fig. 4

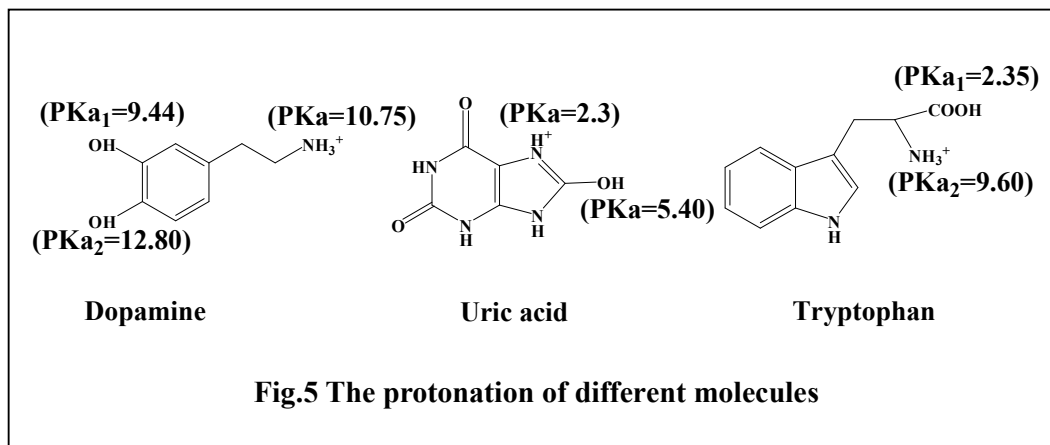


Fig.5

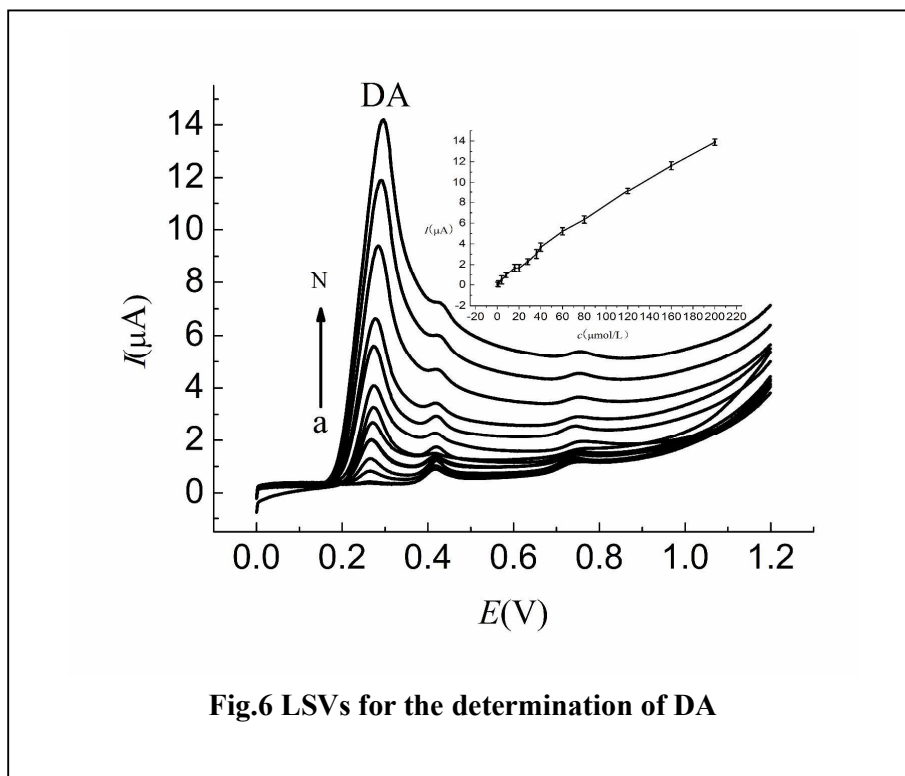


Fig.6

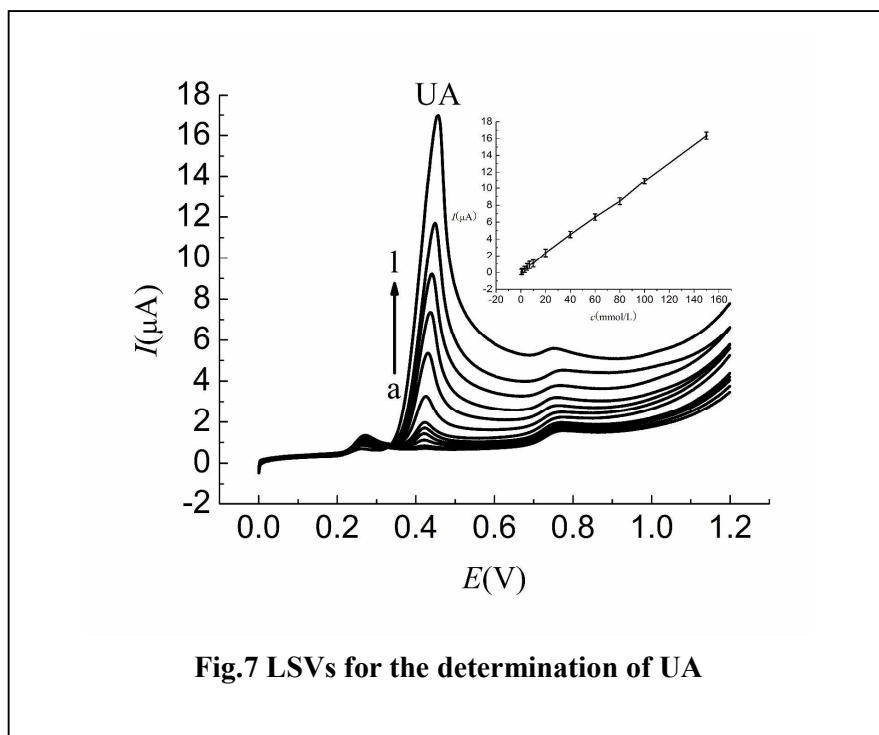


Fig.7

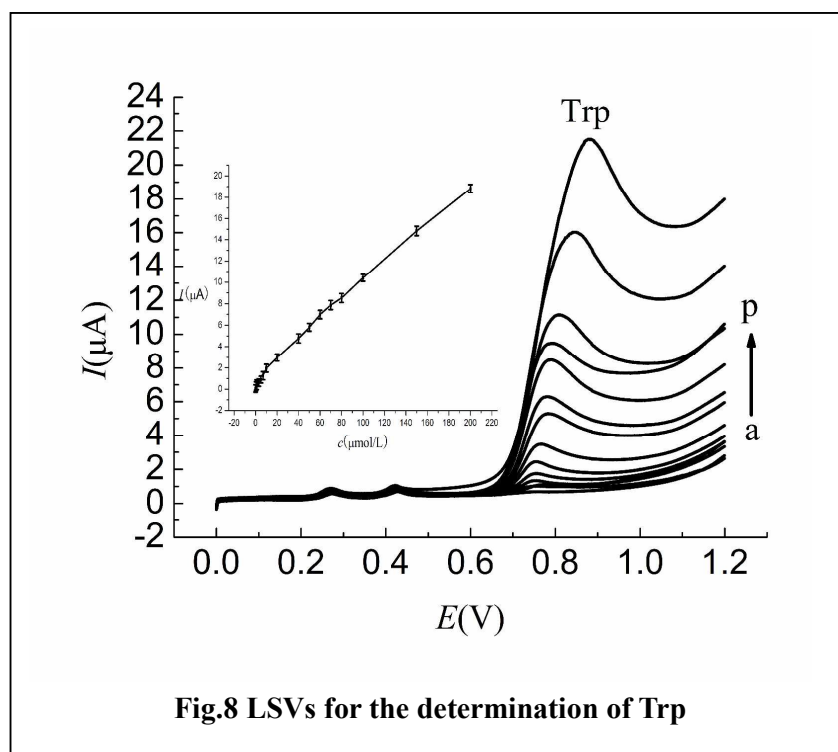
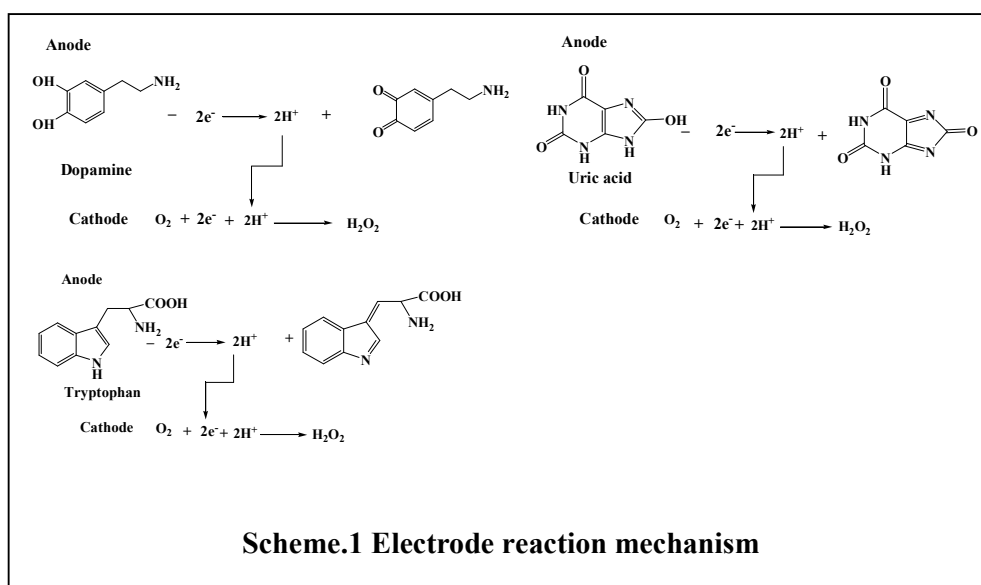


Fig.8

1  
2  
3  
4  
5  
6  
7  
8  
9  
10  
11  
12  
13  
14  
15  
16  
17  
18  
19  
20  
21  
22  
23  
24  
25  
26  
27  
28  
29  
30  
31  
32  
33  
34  
35  
36  
37  
38  
39  
40  
41  
42  
43  
44  
45  
46  
47  
48  
49  
50  
51  
52  
53  
54  
55  
56  
57  
58  
59  
60

### Scheme Legends

**Scheme.1 Electrode reaction mechanism**



1  
2  
3  
4  
5  
6  
7  
8  
9  
10  
11  
12  
13  
14  
15  
16  
17  
18  
19  
20  
21  
22  
23  
24  
25  
26  
27  
28  
29  
30  
31  
32  
33  
34  
35  
36  
37  
38  
39  
40  
41  
42  
43  
44  
45  
46  
47  
48  
49  
50  
51  
52  
53  
54  
55  
56  
57  
58  
59  
60

**Table Legends**

**Table.1**

**Determination of actual samples and recoveries ( $n=5$ ,  $t_{0.05, 4} = 2.58$ )**

**Table.1****Determination of actual samples and recoveries (n=5,  $t_{0.05, 4} = 2.58$ )**

Sample	Measured ( $\mu\text{mol/L}$ )	Added ( $\mu\text{mol/L}$ )	Found ( $\mu\text{mol/L}$ )	Recovery (%)	RSD (%)	
Urine(a)	DA(a)	-	5.00	4.88	97.6	1.4
	UA(a)	37.28	10.00	47.35	100.7	2.2
	Trp(a)	-	5.00	4.96	99.2	3.1
serum(b)	DA(b)	-	5.00	5.05	101.0	2.8
	UA(b)	26.83	10.00	36.48	96.5	4.0
	Trp(b)	3.90	2.00	6.02	106.0	2.4
DA injection(c)	DA(c)	652.8	300.0	953.0	100.1	3.8
	UA(c)	-	5.00	4.96	99.2	3.1
	Trp(c)	-	10.00	10.08	100.8	2.5

“-”: no detected.